Synthesis and Mesomorphic Properties of Main-Chain Polymers Containing V-Shaped Bent-Core Mesogens with Acute-Subtended Angle

ARTICLE *in* MACROMOLECULES · FEBRUARY 2010

Impact Factor: 5.8 · DOI: 10.1021/ma902184s

Macromolecules
ARTICLE

Macromolecules **2010**, *43*, 2865–2872 **2865**
DOI: 10.1021/ma902184s

Synthesis and Mesomorphic Properties of Main-Chain Polymers Containing V-Shaped Bent-Core Mesogens with Acute-Subtended Angle

E-Joon Choi,*,† Eun-Chol Kim,† Chang-Woo Ohk,‡ Wang-Cheol Zin,‡ Ji-Hoon Lee,§ and Tong-Kun Lim§

†*Department of Polymer Science and Engineering, Kumoh National Institute of Technology, Gumi, Gyungbuk 730-701, Korea,* ‡*Department of Material Science and Engineering, Pohang University of Science and Technology, Pohang, Gyungbuk 790-784, Korea, and* §*Department of Physics, Korea University, Seoul 136-713, Korea*

Received October 5, 2009; Revised Manuscript Received February 3, 2010

ABSTRACT: Four achiral polymers with V-shaped bent-core mesogens in the main chain have been synthesized by polycondensation, and the effect of acute-angled central cores (Ar = 1,2-phenylene or 2,3-naphthylene) and lateral halogen substituents (X = F or Cl) was studied. All polymers were only soluble in strong acids such as H_2SO_4 and CF_3CO_2H. The solution viscosities were in the range of 0.31−0.81 dL/g. Although polymers contained a V-shaped bent-core mesogen with acute-angled configuration in their main chain, in general they were semicrystalline in the solid state and could form smectic C phases in the melt state. However, polymer with Ar/X = 1,2-phenylene/Cl was almost amorphous. Especially, polymer with Ar/X = 2,3-naphthylene/F formed a ferroelectric smectic C phase ($SmCP_F$), possibly B7 phase: on ground state the spontaneous polarization was not zero (P_s = 140 nC cm^{-2}), and on applying an triangular electric field a switching occurred by a collective rotation of the mesogens around the main chain axis.

Introduction

The discovery that bent-core molecules can form polar chiral smectic phases opened a new field in liquid crystal research.[1−4] The most attractive aspects of this new class of liquid crystals are in polarity and chirality of mesophases, despite the fact that molecules are nonchiral. Because of the interlayer correlations of three independent stereogenic elements such as chirality (+ or −), clinicity (S: syn; A: anti), and polarity (F: ferro; A: antiferro) in adjacent layers, bent-core molecules can exhibit a much richer variety of smectic and columnar phases than rodlike molecules. The mesophases of bent-core molecules have been named as the code letters B1 to B7 (B stands for banana, bent, bow, or boomerang) according to the order of discovery. The B2 phase is the most extensively studied B phase and is defined as the polar smectic C phase (SmCP) that is subdivided into SmC_SP_A (racemic antiferroelectric), SmC_AP_F (racemic ferroelectric), SmC_AP_A (homochiral antiferroelectric), and SmC_SP_F (homochiral ferroelectric) structures. In particular, B7 phase was defined as the most complex SmC_SP_F phase that is so different from the B2 phase.[5] The B7 phase has attracted attention because of its characteristic optical textures, featuring twisted helical filaments,[2b,6−8] high- and low-birefringence focal conics,[7,9] banana leaf-like domains,[8] checkerboard textures,[2b,7,9,10] and freely suspended filaments.[7,10] It is worth noting that it was proposed that the B7 phase is a polarization modulated/undulated layer stripe structure.[5] In addition, the switching mechanism of bent-core mesogens is more complicate compared with that of calamitic mesogens. In an electric field, dipole moments of bent-core mesogens can adjust their directions to the electric field by two competing switching mechanisms: rotation on the tilt cone around the layer normal or rotation around the long molecular axis.[3b,11]

*Corresponding author: e-mail ejchoi@kumoh.ac.kr; Ph +82-54-4787684; Fax +82-54-4787710.

Regarding five- or six-ring systems, theses bent-core molecules can be classified into two categories according to the bending angle of central core: the V-shaped molecules with acute angled central core or the banana-shaped molecules with obtuse angled central core. The former molecules contain the 1,2-substituted benzene ring as a central core, while the latter molecules contain the 1,3-substituted benzene ring as a central core. In this paper, we focus only on the V-shaped molecules with acute angled central core. Vorländer[12] was a pioneer who reported the first synthesis and masophase behavior of bent-core molecules: as long ago as 1929, he described the liquid crysralline properties of a number of compounds such as bis[4-(4-methoxyphenylazo)phenyl] isophthalate and 1,2-phenylene bis[4-(4-ethoxyphenylazoxy)benzoate] for which he supposed obtuse and acute angled configurations. In 1991, there was renewal of interest in the bent-core molecules based on V-shaped mesogens with Schiff's base linking groups: Kuboshita et al.[13] reported synthesis a series of 1,2-phenylene bis[4-(4-alkoxybenzylideneamino)benzoates], which showed nematic, smectic A, and smectic B phases depending on the length of terminal flexible groups. In 1993, Matsuzaki et al.[14] reported a series of 1,2-phenylene bis[4-(4-alkoxyphenyliminomethyl)benzoates], which also showed nematic, smectic A, and smectic B phases depending on the length of terminal flexible groups. In 2001, Veena Prasad[15] reported synthesis and mesophase behavior of a series of 1,2-phenylene bis[4-(4-alkoxyphenylazo)benzoates]. These compounds with azo-linking groups were found to form nematic, smectic A, and crystal E phases. In 2004, Yelamaggad et al.[16] reported synthesis and mesophase behavior of V-shaped bent-core mesogens with salicylaldimine segments. These compounds with intramolecular hydrogen bonding were found to form nematic and smectic A phases. Recently, V-shaped bent-core mesogens based on 1,2-, 1,3-, 1,7-, and 2,3-dihydroxynaphthalene with Schiff's base linking groups were found to form smectic A and B4 phases.[17] More recently, we found that the V-shaped bent-core mesogens based on 1,7-dihydroxynaphthalene without Schiff's base linking groups was nonliquid crystalline,[18] while the analogue compound

Published on Web 03/01/2010

Scheme 1. Synthetic Route to Polymers with V-Shaped Mesogens

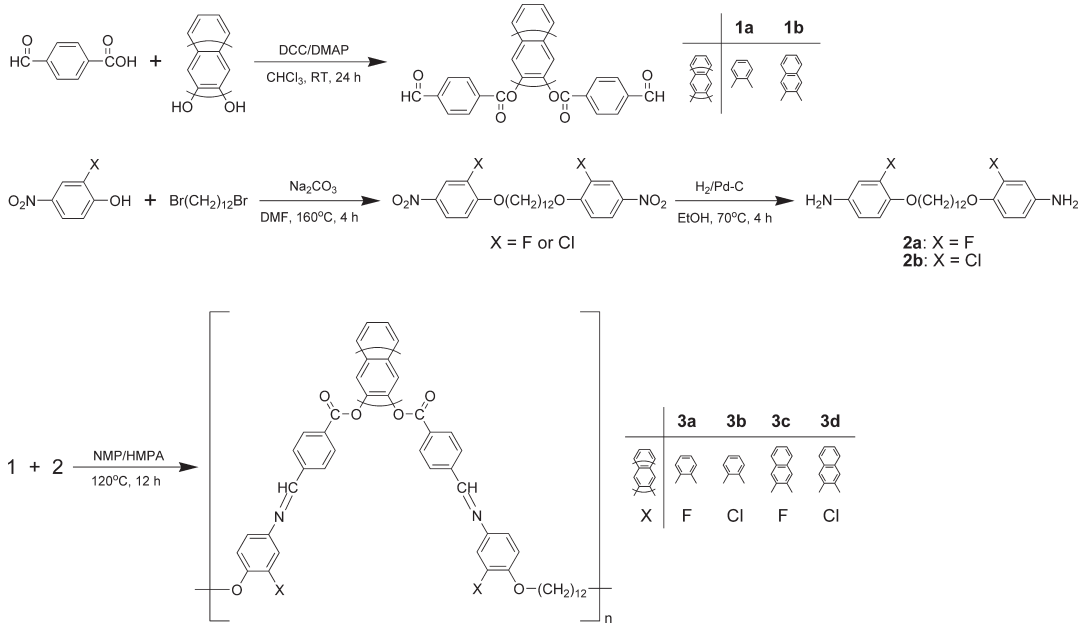

based on 2,3-dihydroxynaphthalene could form nematic and smectic A phases.[19]

Although a considerable number of studies have been made on the structure−property relationships for the bent-core compounds, research on polymers containing bent-core mesogens is still limited. Indeed, the most bent-core monomers have been reported contain mainly methacrylate or vinyl groups in both ends of molecules, sometimes which could be cross-linked to produce network polymers with bent-core mesogens.[20−33] A first side-chain polymer with bent-core mesogens contained polysiloxane as a backbone but mole ratio of mesogens was relatively low to ensure switching behavior.[34] Recently, Chen et al.[35] reported that first side-chain poly(methacrylates) with bent-core mesogens could not switch upon applying an electric field while a weak antiferroelectric switching was observed in a low molecular weight. AB block copolymers containing bent-core and rodlike mesogens were synthesized by alternating diene metathesis polycondensation and found to form a nematic phase.[26,36] The first main-chain polymers containing bent-core mesogens with an obtuse-subtended angle could form B1 and B2 mesophases, but the high viscosity and high phase transition temperature restricted further investigation of electro-optical properties.[37]

In this work, we focused on smectic mesophases formed by main-chain liquid-crystalline polymers with V-shaped bent-core mesogens which have an acute-subtended angle (60°) instead of an obtuse-subtended angle (120°) and the influence of the lateral halogen substituent placed on one of the phenyl rings in the mesogenic unit. We anticipated that such a lateral substituent should encourage an acute-angled mesogen to form a polar smectic mesophase. Four semiflexible polymers containing 1,2-dihydroxyphenylene and 2,3-dihydroxynaphthylene central cores and a lateral F or Cl substituent have been synthesized. Their mesomorphic properties were investigated by differential scanning calorimetry, polarizing optical microscopy, and X-ray diffractometry. In addition, electro-optical investigation was carried out including measurements of switching current response, birefringence, and second harmonic generation (SHG) signal.

Experimental Section

The synthetic route to polymers is shown in Scheme 1. These polymers were prepared according to the synthetic procedures similar to those reported in the literature with minor modification.[37] Since the synthetic procedures used to prepare the polymers were essentially same, one representative polymer (**3a**) is given in the following. All analytical data of the other polymers (**3b**−**3d**) are also included.

Synthesis of Polymer 3a. 1,2-Phenylene bis(4-formylbenzoate) (**1a**) (0.60 g, 1.6 mmol) and 1,12-bis(2-fluoro-4-aminophenoxy)dodecane (**2a**) (0.67 g, 1.6 mmol) were dissolved in 30 mL of dry dichloromethane and evaporated for dryness at 80 °C. The residue was dissolved in a mixture (50 mL) of 1-methyl-2-pyrrolidinone (NMP) and hexamethylphosphoramide (HMPA) (4:1 v/v). The solution was heated to 120 °C with stirring for 12 h. After reaction, the mixture was cooled to ambient temperature and then poured into methanol. The precipitated polymer was washed with water and methanol thoroughly in turn. Yield: 86%. IR (KBr pellet, cm^{-1}): 3060 (aromatic =CH, st), 2922, 2848 (aliphatic C−H, st), 1740 (C═O, st), 1512, 1472 (aromatic C═C, st), 1623 (C═N, st) 1268, 1105, 1061 (C−O, st). ^{1}H NMR spectrum (CF_3CO_2D, δ in ppm): 9.91 (2H, s, N═C*H*), 9.19−7.00 (16H, m, Ar−*H*), 4.15 (4H, d, J = 3.96 Hz, OCH_2), 2.37−2.17 (4H, m, OCH$_2$CH_2), 1.80 (4H, m, OCH$_2$CH$_2$-CH_2). Elemental analysis: $C_{49}H_{52}F_2N_2O_6$ requires C 73.30, N 3.49, H 6.53; found C 72.57, N 4.26, H 6.30%.

Synthesis of Polymer 3b. Polycondensation of **1a** (0.60 g, 1.6 mmol) and **2b** (0.72 g, 1.6 mmol) was carried out following the same procedure as above. Yield: 89%. IR (KBr pellet, cm^{-1}): 3065 (aromatic =CH, st), 2922, 2850 (aliphatic C−H, st), 1741 (C═O, st), 1493, 1464 (aromatic C═C, st), 1622 (C═N, st) 1234, 1162, 1055 (C−O, st). ^{1}H NMR spectrum (CF_3CO_2D, δ in ppm): 9.15 (2H, s, N═C*H*), 8.49−7.06 (16H, m, Ar−*H*), 4.12 (4H, d, J = 5.78 Hz, OCH_2), 2.37−2.17 (4H, m, OCH$_2$CH_2), 1.80 (4H, m, OCH$_2$CH$_2$CH_2). Elemental analysis: $C_{49}H_{52}Cl_2N_2O_6$ requires C 70.41, N 3.35, H 6.27; found C 70.09, N 4.13, H 6.11%.

Synthesis of Polymer 3c. Polycondensation of **1b** (0.68 g, 1.6 mmol) and **2a** (0.67 g, 1.6 mmol) was carried out following the same procedure as above. Yield: 87%. IR (KBr pellet, cm^{-1}): 3052 (aromatic =CH, st), 2915, 2850 (aliphatic C−H, st), 1704 (C═O, st), 1525, 1467 (aromatic C═C, st), 1643 (C═N, st) 1294, 1198, 986 (C−O, st). ^{1}H NMR spectrum (CF_3CO_2D, δ in ppm): 9.97 (2H, s, N═C*H*), 9.15−6.87 (18H, m, Ar−*H*), 4.21 (4H, d, J = 6.21 Hz, OCH_2), 1.85 (4H, d, J = 6.02 Hz, OCH$_2$CH_2), 1.29 (4H, m, OCH$_2$CH$_2$CH_2). Elemental analysis: $C_{53}H_{54}F_2N_2O_6$ requires C 74.63, N 3.28, H 6.38; found C 71.27, N 4.81, H 6.72%.

Table 1. General and Thermal Properties of Polymers

polymer (Ar/X)	yield (wt %)	η_{inh}[a] (dL/g)	DSC scan	T_g (°C)	T_{k-k} (°C)	T_m (°C)	ΔH_m[d] (kJ/mol)	T_c (°C)	ΔH_c (kJ/mol)	T_i (°C)	ΔH_i (kJ/mol)	T_d (°C)	residue at 600 °C (wt %)
3a (1,2-Ph/F)	86	0.31	heating			115	55.2			182	2.9	302	52.4
			cooling							179	2.8		
			b			109	23.2			182	2.1		
3b (1,2-Ph/Cl)	89	0.40	heating	53		147	1.5			181	1.5	303	50.7
			cooling	57						168	1.6		
			b	61						179	1.5		
3c (2,3-Naph/F)	87	0.81	heating		182	202	76.6			e		411	41.8
			cooling					158	47.2	e			
			c		195	201	40.1			e			
3d (2,3-Naph/Cl)	86	0.62	heating		191	198	97.3			e		381	42.9
			cooling					161	32.3	e			
			c		179, 189	201	34.0			e			

[a] Inherent viscosity was measured in 0.16 g/dL solution of H_2SO_4 at 30 °C. [b] The second heating after previous thermal treatment at 200 °C. [c] The second heating after previous thermal treatment at 250 °C. [d] Total enthalpy changes for the T_{k-k} and T_m transitions. [e] Thermal decomposition occurred before isotropization.

Synthesis of Polymer 3d. Polycondensation of **1b** (0.68 g, 1.6 mmol) and **2b** (0.72 g, 1.6 mmol) was carried out following the same procedure as above. Yield: 86%. IR (KBr pellet, cm^{-1}): 3054 (aromatic =CH, st), 2918, 2850 (aliphatic C−H, st), 1704 (C=O, st), 1503, 1467 (aromatic C=C, st), 1646 (C=N, st) 1255, 1198, 986 (C−O, st). ^1H NMR spectrum (CF_3CO_2D, δ in ppm): 9.98 (2H, s, N=C*H*), 9.14−7.04 (18H, m, Ar−*H*), 4.18 (4H, d, OCH_2), 2.87 (4H, d, J = 9.61 Hz, OCH_2CH_2), 1.81 (4H, m, $OCH_2CH_2CH_2$). Elemental analysis: $C_{53}H_{54}Cl_2N_2O_6$ requires C 71.85, N 3.16, H 6.14; found C 67.81, N 6.19, H 6.90%.

Instruments. IR and NMR spectra were obtained by a Jasco 300E FT/IR and a Bruker DPX 200 MHz NMR spectrometer. Elemental analysis was performed with a Thermofinnigan EA1108. The transition behaviors were characterized by a differential scanning calorimetry (Netzsch DSC 200 F3 Maia). DSC measurements were performed in a N_2 atmosphere with heating and cooling rates of 10 °C/min. Optical texture observation was carried out using the polarizing microscope (Zeiss, Jenapol and Axioskop 40 Pol) with a heating stage (Mettler FP82HT). Thermal stability of polymers was measured by DuPont TGA 2950 under a N_2 atmosphere with a heating rate of 20 °C/min. Solution viscosities of obtained polymers were measured at 30 °C using a Ubbelohde-type viscometer.

X-ray Investigation. XRD measurements were performed in transmission mode with synchrotron radiation (λ = 1.54 Å) at the Pohang Accelerator Laboratory (PAL) in Korea. The sample sealed with a window of 7 μm thick Kapton film on both sides was held in an aluminum sample holder. The data are presented as a function of $q = 4\pi \sin \theta/\lambda$ (θ: the scattering angle). The sample was heated with two cartridge heaters, and its temperature was monitored by a thermocouple placed close to the sample. A background scattering correction was performed by subtracting the scattering from the Kapton film.

Electrooptical Measurement. Each ITO deposited substrate was spin-coated with a commercial polyimide solution of AL1254 (JSR Corp.) and was baked for 1 h at 230 °C. The rubbing directions of the upper and the lower substrates were antiparallel to each other. The cell gap was kept at 2 μm by ceramic bead spacer with 2 μm diameter. The size of the electrode area was 2 cm × 2 cm. LC polymer was dropped onto lower substrate which was heated up to the transition temperature T_{NI}. Then, the upper slide was put down and attached by UV-curable epoxy. It showed imperfect alignment; therefore, the signal-to-noise ratio was relatively high. However, it still was possible to investigate electro-optical switching behavior by using a lock-in amplifying technique. A He−Ne laser (632 nm) was used to examine the switching behavior of the optic axis of the cell. For the second harmonic generation (SHG) measurements, a Q-switched ND-YAG pulse laser (GCR-200, Spectra Physics, 1064 nm, 7 ns pulse width, 10 Hz repetition rate) was used; the experimental setup was similar to one reported in the literature.[38] The temperature of the sample was maintained using a heating stage (TMS94, Linkam).

Results and Discussion

Synthesis and Mesogenic Properties. We have synthesized four azomethine polymers to realize our motif toward smectic phases in the main-chain polymers with acute-angled bent-core mesogens. The synthetic route for poly(azomethines) is quite straightforward, and each reaction step is a relatively well-known type, except that a mixture of NMP/HMPA (4:1 v/v) was used as a cosolvent for the polycondensation.[37] Once products were obtained as a precipitate, polymers were only soluble in strong acids such as H_2SO_4 and CF_3CO_2H. In Table 1, the yields of polymers were in the range of 86−89%. This means that the low molecular weight portions were considerably removed during the precipitation process after polymerization reaction. However, the elemental analysis results indicate that polymers still contain non-negligible amounts of low molecular weight portions with amide or aldehyde end groups. The structures of polymers with ester, azomethine, and ether linkages were characterized by IR and NMR spectroscopy. The spectral data were in accordance with the expected formula. The solution viscosities of the polymers were measured by using a 0.16 g/dL solution of sulfuric acid at 30 °C. Although the solution was accompanied by an appreciable degree of decomposition, the inherent viscosity (η_{inh}) numbers were tolerable in the range of 0.31−0.81 dL/g.

Figure 1 shows the DSC thermograms of polymers. Polymer **3a** shows two endothermic peaks for melting and isotropization during heating and only an exothermic peak for reversible isotropization during cooling; a crystallization was found just before the melting. Polymer **3b** shows an inflection for glass transition and a peak for isotropization during cooling and heating, except that a minute melting endotherm was found in the first heating curve. Polymers **3c** and **3d** show a multiple melting during heating and a supercooling of recrystallization during cooling. Their isotropization temperatures could not be defined because thermal decomposition occurred before the transition. The transition temperatures and enthalpy changes defined by DSC are summarized in Table 1. The enthalpy change for isotropization (ΔH_i) of polymer **3a** was about 2 times greater than the ΔH_i of polymer **3b**. This implies that the fluorine atom can bestow better mesogenic property due to higher electron negativity, lower molecular cohesive energy, and smaller van der Waals radius compared with the chlorine atom. Polymers **3c** and **3d** with a 2,3-naphthalene central core have much higher T_m and T_i values than polymers **3a** and **3b** with a

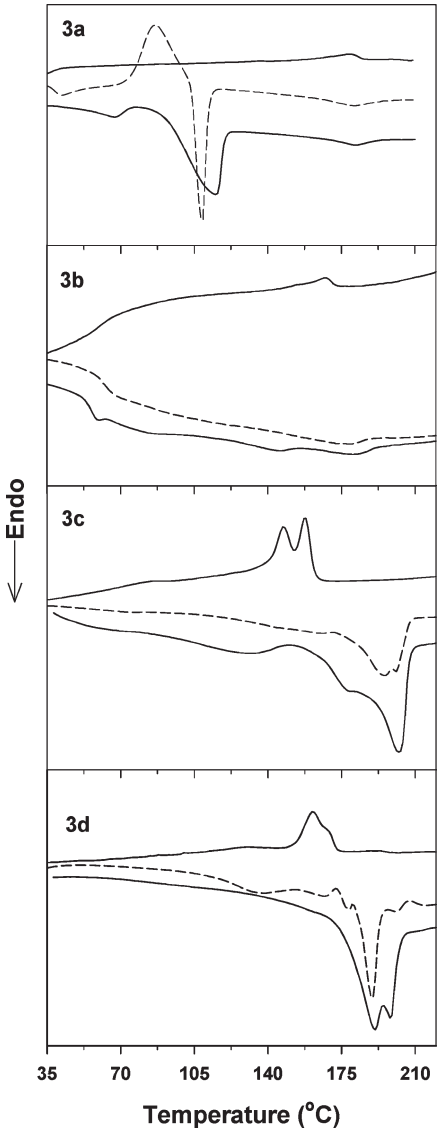

Figure 1. DSC thermograms of polymers at a rate of 20 °C/min: the lower thin line, the first heating; the middle broken line, the second heating; the upper thin line, the first cooling.

1,2-phenylene central core. We suppose that the second ring extruded in the 2,3-naphthylene central core plays an important role in enhancing packing and directional ordering of mesogens, instead of revealing a steric hindrance. However, the amorphous behavior of polymer **3b** can be attributed to the coexistence of a bulky chlorine atom and a highly bent 1,2-phenylene central core.

Figure 2 shows the TGA curves of polymers. Although polymers **3c** and **3d** show the two-stage weight loss, degradation temperature (T_d) of the polymers should be higher than 300 °C. We speculate the first weight loss at about T_m is due to non-negligible amount of oligomers which start vaporization around the T_m. In practice, we found that for polymers **3c** and **3d** the heat of melting (ΔH_m) during the second heating was almost equivalent with the heat of recrystallization (ΔH_c). Nevertheless, the lower ΔH_m for polymer **3a** during the second heating than during the first heating can be attributed to a melting hysteresis.

Figure 3 shows cross-polarizing optical micrographs obtained using a normal glass substrate. Phases could be confirmed by combination of optical microscopic observation, X-ray diffractometry, and electro-optical measurement. The

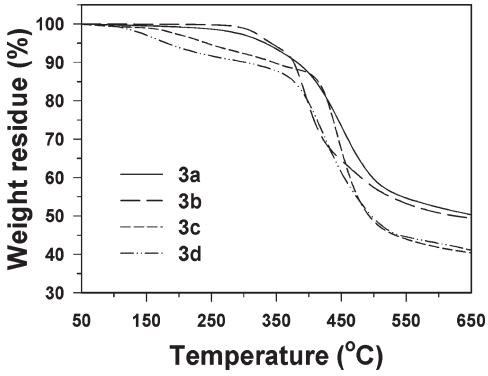

Figure 2. TGA thermograms of polymers at a heating rate of 20 °C/min.

smectic C phase of polymer **3a** showed a schlieren texture with singularities during heating (Figure 3a) and one with inversion lines during cooling (Figure 3b). The solid state of polymer **3b** was almost nonbirefringent (Figure 3c), and on heating to 170 °C the smectic phase showed distinctively birefringence even without a typical optical texture (Figure 3d), perhaps due to its unique layer structure with relatively poor orderness. As further heated to 178 °C, the brightness somewhat decreased (Figure 3e). Finally, a dark state of isotropic liquid phase was found at 184 °C (Figure 3f). During heating polymer **3c** showed a banana leaf-like domain (left upper portion of Figure 3k) and seems to show a twisted helical filament (lower portion horizontally crossed in Figure 3k), suggesting B7 phase; during cooling a filament-like texture was grown in from the isotropic phase (Figure 3g), which was transformed into a broken fan-like texture (Figure 3h,i), and at 112 °C a texture of solid state with paramorphosis was found (Figure 3j). Polymer **3d** shows a broken fan texture of smectic C phase (Figure 3l).

X-ray Diffraction Studies. Figure 4 shows the synchrotron radiation X-ray diffraction (XRD) patterns of polymers at the given temperatures. The sample used for X-ray measurement was prepared by precipitation from the nonsolvent and kept under vacuum for 5 days. In the first heating run the X-ray diffraction pattern of polymer **3a** shows the crystal-like wide-angle diffraction peaks at room temperature. As heated to 90 °C, the diffraction peaks become stronger, suggesting the solid-state crystallization. On heating to 160 °C, only a broad but strong peak at $q = 2.42$ nm^{-1} appears in the small angle region while all peaks in wide angle region disappeared. This is indicative of a smectic phase. But it was reported that the similar profile of X-ray scattering was originated from a nematic phase.[39] However, we could exclude the possibility of the nematic phase because the *d*-spacing of such smectic phase was far different from the nematic phase (4.3 nm). As further heated to 210 °C, only a broad scattering appears, indicating an isotropic liquid phase. Subsequently, as the liquid phase was cooled to 120 °C, a sharp peak appears at $q = 2.48$ nm^{-1}. Clearly this is indicative of a smectic phase with $d = 2.53$ nm, which was monotropic. Even by cooling to room temperature, diffraction peaks in the wide angle region were not recovered, while in the small angle region the peak for the smectic layer was maintained. This means that the smectic structure can be generated by simple cooling of the isotropic liquid by 10 °C/min to room temperature even though it was not rapid cooling. The similarity is shown by DSC. When the sample is cooled by 20 °C/min after melting, the crystallization exothermic peak does not appear on cooling. But, the DSC shows the recrystallization peak around 90 °C and the melting peak around 110 °C in the second run.

Polymer **3b** shows only a board but strong peak in the small angle region at room temperature and 80 °C. On heating

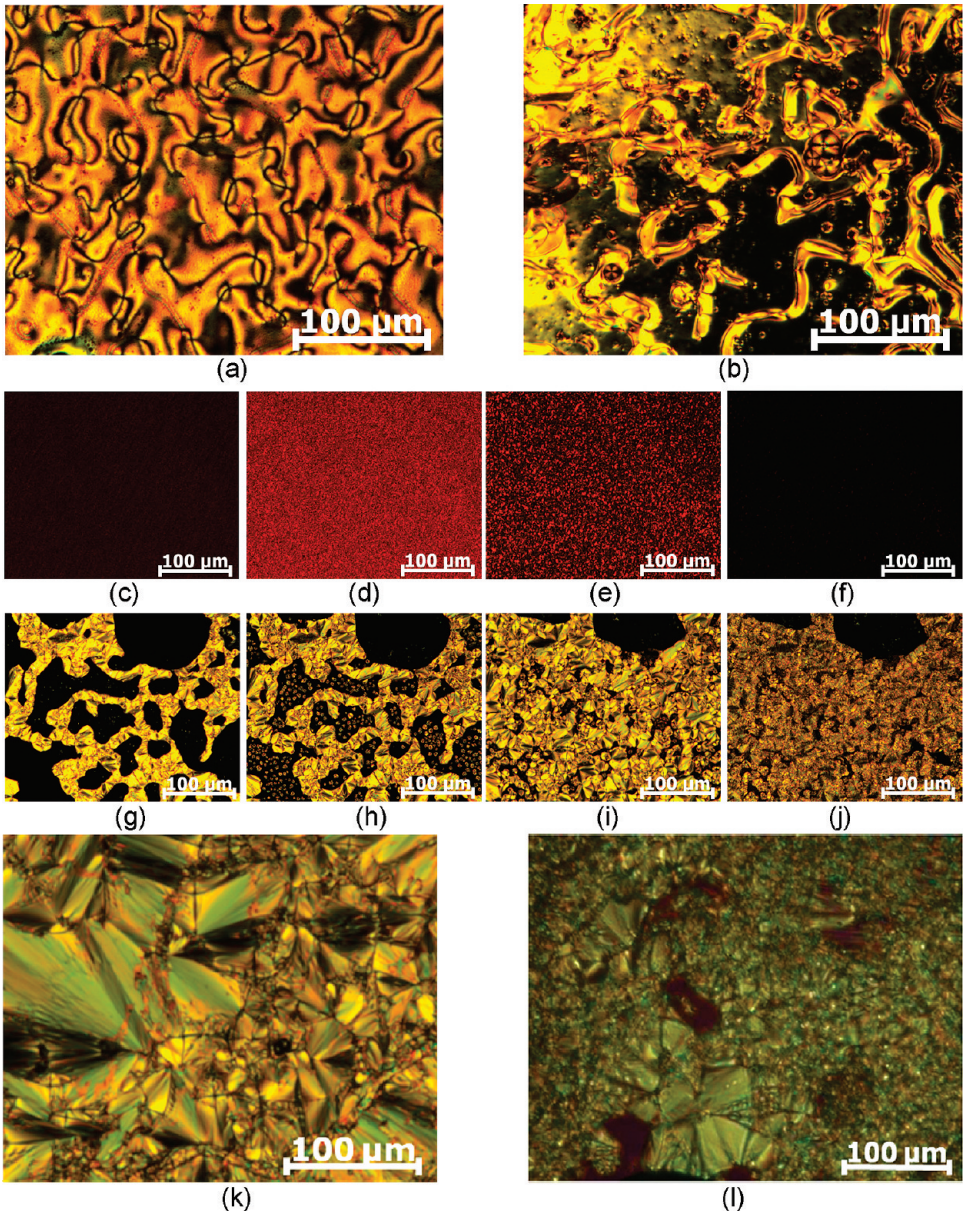

Figure 3. Cross-polarizing optical micrographs of polymers (magnification 200× except for **3d**): **3a**, (a) on the second heating T = 171 °C, (b) on cooling T = 132 °C; **3b**, during the second heating (c) T = 96 °C, (d) T = 170 °C, (e) T = 178 °C, (f) T = 184 °C; **3c** (the upper black region is an empty place), during cooling (g) T = 255 °C, (h) T = 241 °C, (i) T = 166 °C, (j) T = 112 °C; (k) on the second heating T = 203 °C; (l) **3d**, on heating T = 291 °C (250×).

to 160 °C, the peak becomes weaker. This indicates that polymer **3b** is almost amorphous in solid state and can form a smectic phase with d = 2.54 nm in melt state, but orderness of layer structure is not good. As further heated to 210 °C (higher than the T_i of 181 °C defined by DSC), the polymer shows only a diffused scattering, indicating the isotropic phase. When the liquid phase was cooled to 130 °C, a peak of smectic phase with d = 2.58 nm appeared. On cooling to room temperature, in the small angle region only a broad peak appears. This means that only an amorphous state without the smectic layer structure was obtained by cooling to room temperature.

Polymer **3c** shows many diffraction peaks at room temperature and 140 °C. The X-ray scattering intensity from an ideal two-phase lamellar structure is obtained at a series of q values satisfying $q = 2\pi n/d$, where d is lamellar thickness, and the height of the nth-order peak is proportional to $\sin^2(\pi n\Phi_A)/n^2$, where Φ_A is the volume fraction of phase A. In polymer **3c** the ratio of peak position is 1:2:4. The missing of third-order peak means that the volume ratio of the A and B phases is 1:2. The molar masses of rod and coil parts are 640 and 168, respectively. Considering the crystalline state in rod part and liquid state in coil part at room temperature, the density of rod and coil part could be assumed by 1.5 and 0.8, respectively. Then the calculated volume ratio of rod and coil parts is very close to 2:1. On heating to 230 °C (higher than the T_m of 202 °C defined by DSC), two peaks were found in the small angle region and a peak (q = 18.47 nm^{-1}) in the wide angle region. As further heated to 270 °C, a typical diffraction pattern of smectic phase was observed: the two peaks remained in small angle region but no peaks in wide angle region. Subsequently, when the smectic phase was cooled to 200 °C (not lower than T_c of 158 °C defined by DSC), in addition to the peaks in the small angle region, a few peaks appeared in the wide angle region. As further cooled to 120 °C and room temperature, three peaks with the ratio

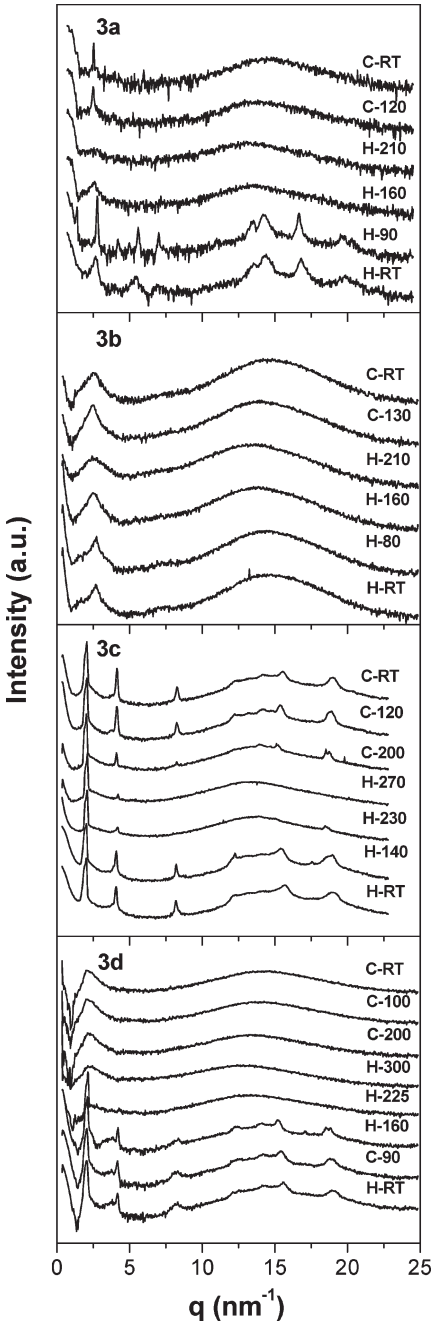

Figure 4. Synchrotron radiation X-ray diffraction patterns of polymers at the given temperatures. Abbreviations: RT = room temperature; H = heating; C = cooling.

of 1:2:4 in the small angle region and several peaks in the wide angle region were found. This means that the crystalline as well as smectic structures formed in the as-polymerized sample were reversibly obtained by cooling the mesophase to room temperature. However, at present we are uncertain whether the diffraction peaks in the wide angle region at 230 °C on heating and 200 °C on cooling (the temperature deviation between DSC and XRD data) would be originated from the formation of a high melting polymorph by further crystallization in solid state or postpolymerization in melt state. Note that on heating from room temperature to 140 °C, *d*-spacing increased from 3.05 to 3.11 nm, and then *d*-spacing was recovered to 3.05 nm at 230 °C and finally decreased to 3.00 nm at 270 °C, and vice versa during cooling.

Table 2. Comparison of Molecular Length (*L*), *q* Value, Layer Spacing (*d*), and Tilt Angle (θ) for Smectic Phases

polymer	measuring temperature (°C)	L^a (nm)	q^b (nm^{-1})	*d* (nm)	θ^c (deg)
3a	H-160	3.58	2.59 (b, s)	2.42	47
	C-120		2.48 (s)	2.53	45
3b	H-160	3.53	2.47 (b, s)	2.54	44
	C-130		2.43 (b, s)	2.58	43
3c	H-230	3.50	2.06 (vs)	3.05	29
	H-270		2.09 (vs)	3.00	31
	C-200		2.06 (vs)	3.05	29
3d	H-225	3.45	2.13 (vs)	2.95	31

[a] The length of molecule with the all-trans conformation was calculated by using the PCFF force-field model of material studio. [b] Abbreviation of the relative intensity: b: broad; s: strong; vs: very strong. [c] The tilt angle was calculated by assuming that the bent angle is 60°, and there is no intercalation between chains.

Polymer **3d** follows the same characters as polymer **3c** before melting in the first heating: many diffraction peaks were found at room temperature, 90 °C and 160 °C, indicating a crystalline structure. On heating to 225 °C, only a sharp peak appears at $q = 2.13\ nm^{-1}$ with $d = 2.95$ nm in the small angle region, indicating a smectic phase. As further heated to 300 °C, only a broad peak was found in the small angle region, suggesting the isotropic phase. However, during cooling the isotropic phase to room temperature, no distinct peaks were found in small as well as wide angle regions. We assumed that if polymer **3d** was not decomposed at 300 °C, the XRD patterns would be similar to those of polymer **3c**: the peaks for crystalline as well as mesomorphic states formed on heating run would appear reversibly during the cooling run.

In Table 2, by assuming the molecular chain to be fully extended in the all-trans-conformation, the length of bent-core mesogen can be calculated to be in the range of 3.45−3.58 nm. Thus, from the *d* values obtained in X-ray data, the tilt angles (θ) of the mesogen normal to the layer can be estimated to be in the range of 29°−47° depending on the structure. Note that the tilt angle of polymers with Ar = 2,3-naphthylene was smaller than that of polymers with Ar = 1,2-phenylene.

Electro-Optical Investigations. Detailed electro-optical investigations carried out on polymers **3a**, **3c**, and **3d** and in general the electro-optical behavior of polymers **3a** and **3d** were the same. For these measurements, the glass substrates with indium tin oxide (ITO) electrodes coated with polyimide and rubbed antiparallel to each other were used. Figure 5 shows the SHG signals upon irradiation of a laser beam. When the P/S polarized probe beam struck the *xz* plane with an incident angle of 60°, polymer **3c** exhibits the strong SHG signals but polymer **3a** no SHG signal: P and S stand for the parallel and the perpendicular polarization, respectively, with regard to the plane including the incident and the reflected beams. In Figure 6a,b no SHG signal regardless of zero or applied voltage implies that dipoles of polymer **3a** are completely compensated, and the macroscopic polarization becomes zero. However, possibility of antiferroelectric response for polymer **3a** should be excluded on the base of following results of electro-optical measurements. By contrast, Figure 6c,d exhibiting strong signal regardless of zero or applied voltage implies that polymer **3c** has a net polarization because the symmetry of mesophase is broken by the ferroelectric arrangement of molecules. Figure 6 shows the dependence of electric field on the SHG signals for polymer **3c**, which were obtained as PP polarization showing the strongest SHG intensity is applied. At zero-field state the SHG intensity was nonzero. When the voltage of electric field increased, the SHG intensity increased gradually

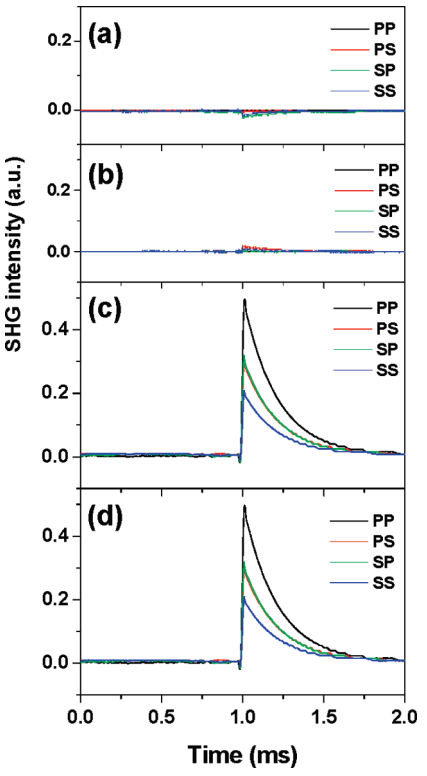

Figure 5. SHG signals by irradiation of P/S polarized probe beam with an incident angle of 60°: (a) **3a**, T = 165 °C, E = 0 V; (b) **3a**, T = 165 °C, E = 30 V; (c) **3c**, T = 215 °C, E = 0 V; (d) **3c**, T = 215 °C, E = 30 V.

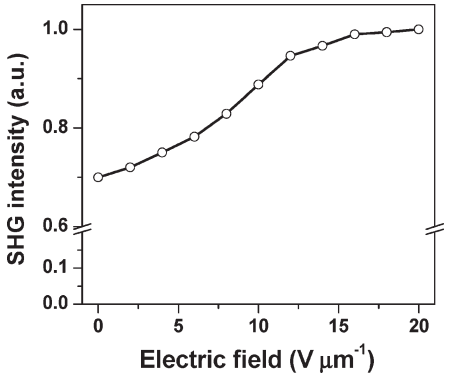

Figure 6. SHG intensity for polymer **3c** as a function of an applied electric field (T = 215 °C).

without a threshold voltage, and then it was almost saturated at 20 V μm^{-1}. The results imply that the ferroelectric ground state of polymer **3c** possesses the field-independent SHG, and as the electric field increases, the uniformity of dipole alignment along the field direction increases gradually.

Figure 7 shows triangular voltage dependence of switching current response. Upon application of a triangular voltage, polymer **3a** shows no switching current response (Figure 7a), whereas polymer **3c** shows a single switching current peak per every half period, suggesting a ferroelectric ground state (Figure 7b). From the current response, the spontaneous polarization (P_s) was calculated to be about 140 nC cm^{-2}. From the results, we can confirm that polymer **3a** does not show an antiferroelectric switching, but polymer **3c** exhibits a ferroelectric switching.

Figure 8 shows the optical transmittance measured as a function of the rotation angle of a set of crossed polarizers. The probe beam was normally incident, and the output beam

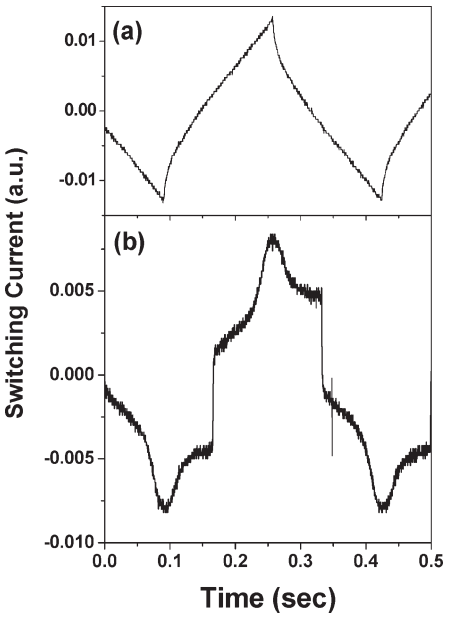

Figure 7. Switching current response on applying a triangular-wave voltage (E = 30 V μm^{-1}, f = 3 Hz): (a) **3a**, T = 160 °C; (b) **3c**, T = 215 °C.

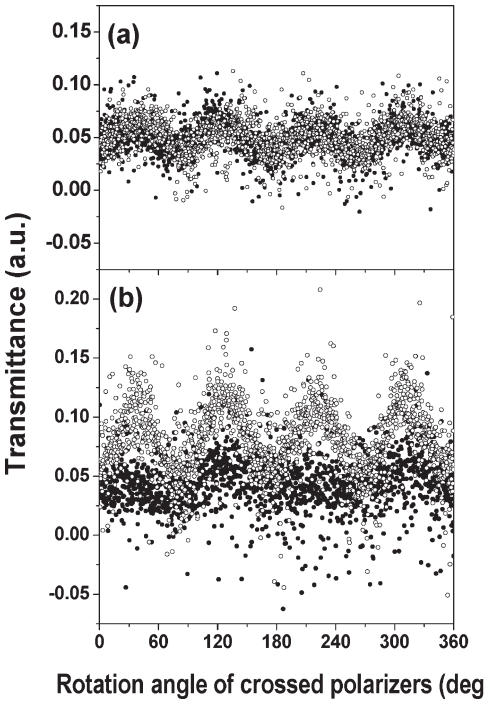

Figure 8. Optical transmittance as a function of the rotation angle of the crossed polarizers at field-off state (●) and under application of an electric field of 15 V μm^{-1} (○): (a) **3a**, T = 160 °C; (b) **3c**, T = 215 °C.

intensity was measured while a set of crossed polarizers is rotating. Initially, the polarization direction of the probe beam was parallel to the rubbing direction: this corresponds to the x = 0 in the figure. At field-off state as well as field-on state, the minimum transmittance was observed at the angle of 0° and the maximum transmittance at the angle of ±45°. When the ac field of 15 V μm^{-1} was applied to the cell of polymer **3c**, the transmittance at the maximum angle increased without change of the rotation angle (Figure 8b). However, upon application of the field polymers **3a** showed neither change of transmittance nor rotation angle (Figure 8a).

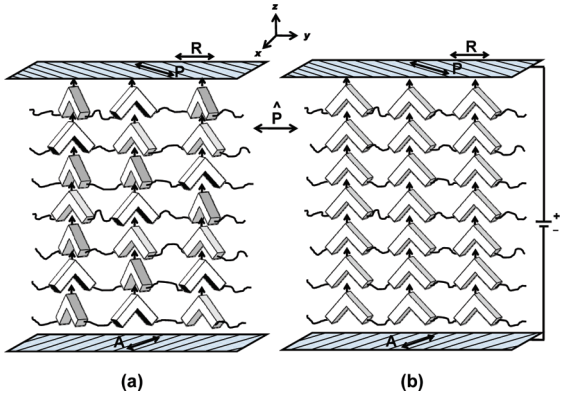

Figure 9. Schematic representation of smectic A structure of polymer **3c**: (a) field-off state; (b) field-on state. Abbreviations: $\hat{p}$ = the layer normal; P = polarizer direction; A = analyzer direction; R = rubbing direction.

From the results of electro-optical measurements, we can propose the possible alignment structure of smectic phase for polymer **3c**: in the molecular frame, the dipoles of mesogens are aligned vertical to the long molecular axis; in the laboratory frame the directors of mesogens are aligned parallel to the rubbing direction (Figure 9). In practice, on the ground state, the director cannot be completely uniformly aligned along the rubbing direction because the tendency of main chain toward statistically stable conformation competes with the tendency of director toward anisotropic orientation along the rubbing direction. When the strength of an electric field applied increases, the mesogens can gradually overcome tendency of main chain toward stable conformation so that the uniformity of dipole alignment increases gradually. Moreover, when a triangular voltage applied, a polar switching occurred by a collective rotation of the molecules around their main chain axes.

Conclusions

In summary, four achiral main-chain polymers containing V-shaped bent-core mesogens with acute-angled central cores (Ar = 1,2-phenylene or 2,3-naphthylene) and lateral halogen substituents (X = F or Cl) have been synthesized and characterized. In spite of existence of the acute-angled central cores, only one polymer with Ar/X = 1,2-phenylene/Cl was almost amorphous (T_g = 53−61 °C), and the remaining three polymers were semicrystalline (T_m = 109−202 °C). Although polymers contain V-shaped mesogens, all polymers with a lateral halogen substituent could form tilted smectic phases (d = 2.42−3.05 nm, θ = 29°−47°), i.e., smectic C phases. Moreover, polymer with Ar/X = 2,3-naphthalene/F could form a ferroelectric smectic C phase: on ground state the spontaneous polarization of smectic phase was not zero (P_s = 140 nC cm^{-2}) and on applying a triangular voltage the switching occurred by a collective rotation of the mesogens around main chain axis. Based on the optical textures observed, the polar smectic C phase with the ferroelectric ground state ($SmCP_F$) may be regarded as B7 phase. However, without direct experimental evidence for the modulation structures[5] by X-ray analysis, more studies are needed to confirm this.

Acknowledgment. This work was supported by the Korea Science and Engineering Foundation (KOSEF) grant funded by Korea government (MEST) (No. R01-2008-000-11521-0).

References and Notes

(1) (a) Niori, T.; Sekine, T.; Watanabe, J.; Furukawa, T.; Takezoe, H. *J. Mater. Chem.* **1996**, *6*, 1231. (b) Takezoe, H.; Takanishi, Y. *Jpn. J. Appl. Phys.* **2006**, *45*, 597.
(2) (a) Link, D. R.; Natale, G.; Shao, R.; Maclennan, J. E.; Clark, N. A.; Körblova, E.; Walba, D. M. *Science* **1997**, *278*, 1924. (b) Walba, D. M.; Körblova, E.; Shao, R.; Maclennan, J. E.; Link, D. R.; Glaser, M. A.; Clark, N. A. *Science* **2000**, *288*, 2181.
(3) (a) Pelzl, G.; Diele, S.; Weissflog, W. *Adv. Mater.* **1999**, *11*, 707. (b) Weissflog, W.; Dunemann, U.; Schröder, M. W.; Diele, S.; Pelzl, G.; Kresse, H.; Grande, S. *J. Mater. Chem.* **2005**, *15*, 939.
(4) (a) Tschierske, C. *J. Mater. Chem.* **1998**, *8*, 1485. (b) Tschierske, C. *J. Mater. Chem.* **2001**, *11*, 2647. (c) Tschierske, C. *Annu. Rep. Prog. Chem., Sect. C: Phys. Chem.* **2001**, *97*, 191. (d) Amarantha Reddy, R.; Tschierske, C. *J. Mater. Chem.* **2006**, *16*, 907.
(5) (a) Coleman, D. A.; Fernsler, J.; Chattham, N.; Nakata, M.; Takanishi, Y.; Körblova, E.; Link, D. R.; Shao, R. F.; Jang, W. G.; Maclennan, J. E.; Mondainn-Monval, O.; Boyer, C.; Weissflog, W.; Pelzl, G.; Chien, L. C.; Zasadzinski, J.; Watanabe, J.; Walba, D. M.; Takezoe, H.; Clark, N. A. *Science* **2003**, *301*, 1204. (b) Coleman, D. A.; Jones, C. D.; Nakata, M.; Clark, N. A.; Walba, D. M.; Weissflog, W.; Fodor-Csorba, K.; Watanabe, J.; Novotna, V.; Hamplova, V. *Phys. Rev. E* **2008**, *77*, 021703.
(6) Lee, C. K.; Chien, L. C. *Liq. Cryst.* **1999**, *26*, 609.
(7) Pelzl, G.; Diele, S.; Jakli, A.; Lischka, Ch.; Wirth, I.; Weissflog, W. *Liq. Cryst.* **1999**, *26*, 135.
(8) Jákli, A.; Lischka, C.; Weissflog, W.; Pelzl, G.; Saupe, A. *Liq. Cryst.* **2000**, *27*, 1405.
(9) Bedel, J. P.; Rou Rouillon, J. C.; Marcerou, J. P.; Laguerre, M.; Nguyen, H. T.; Achard, M. F. *Liq. Cryst.* **2000**, *27*, 1411.
(10) Jakli, A.; Krüerke, D.; Nair, G. G. *Phys. Rev. E* **2003**, *67*, 051702.
(11) Gorecka, E.; Vaupotic, N.; Pociecha, D.; Cepic, M.; Mieczkowski, J. *ChemPhysChem* **2005**, *6*, 1087.
(12) (a) Vorländer, D. *Ber. Dtsch. Chem. Ges.* **1929**, *62*, 2831. (b) Vorländer, D.; Apel, A. *Ber. Dtsch. Chem. Ges.* **1932**, *65*, 1101.
(13) Kuboshita, M.; Matsunaga, Y.; Matsuzaki, H. *Mol. Cryst. Liq. Cryst.* **1991**, *199*, 319.
(14) Matsuzaki, H.; Matsunaga, Y. *Liq. Cryst.* **1993**, *14*, 105.
(15) Prasad, V. *Liq. Cryst.* **2001**, *28*, 145.
(16) Yelamaggad, C. V.; Shashikala, I.; Shankar Rao, D. S.; Krishna Prasad, S. *Liq. Crst.* **2004**, *31*, 1027.
(17) Lee, S. K.; Naito, Y.; Shi, L.; Tokita, M.; Takezoe, H.; Watanabe, J. *Liq. Cryst.* **2007**, *34*, 935.
(18) Choi, E-J.; Cui, X.; Zin, W.-C.; Ohk, C.-W.; Lim, T.-K.; Lee, J.-H. *ChemPhysChem* **2007**, *8*, 1919.
(19) Choi, E-J.; Cui, X.; Ohk, C.-W.; Zin, W.-C.; Lee, J.-H.; Lim, T.-K.; Jang, W.-G. *J. Mater. Chem.*, DOI: 10.1039/b919404e.
(20) Keum, C. D.; Kanazawa, A.; Ikeda, T. *Adv. Mater.* **2001**, *13*, 321.
(21) Lee, C. K.; Kwon, S. S.; Shin, S. T.; Choi, E-J.; Lee, S.; Chien, L. C. *Liq. Cryst.* **2002**, *29*, 1007.
(22) Fodor-Csorba, K.; Vajda, A.; Galli, G.; Jakli, A.; Demus, D.; Holly, S.; Gacs-Baitz, E. *Macromol. Chem. Phys.* **2002**, *203*, 1556.
(23) Sentman, A. C.; Gin, D. L. *Angew. Chem., Int. Ed.* **2003**, *42*, 1815.
(24) Kwon, S. S.; Kim, T. S.; Lee, C. K.; Shin, S. T.; Oh, L. T.; Choi, E-J.; Kim, S. Y.; Chien, L. C. *Bull. Korean Chem. Soc.* **2003**, *24*, 274.
(25) Barbera, J.; Gimeno, N.; Monreal, L.; Pinol, R.; Ros, M. B.; Serrano, J. L. *J. Am. Chem. Soc.* **2004**, *126*, 7190.
(26) Fodor-Csorba, K.; Jakli, A.; Galli, G. *Macromol. Symp.* **2004**, *218*, 81.
(27) Fodor-Csorba, K.; Vajda, A.; Jakli, A.; Slugovc, C.; Trimmel, G.; Demus, D.; Gacs-Baitz, E.; Holly, S.; Galli, G. *J. Mater. Chem.* **2004**, *14*, 2499.
(28) Lee, C. K.; Kwon, S. S.; Kim, T. S.; Shin, S. T.; Chow, H.; Choi, E-J.; Kim, S. Y.; Zin, W. C.; Kim, D. C.; Chien, L. C. *Bull. Korean Chem. Soc.* **2004**, *25*, 1171.
(29) Novotna, V.; Hamplova, V.; Kaspar, M.; Glogarova, M.; Pociecha, D. *Liq. Cryst.* **2005**, *32*, 1115.
(30) Achten, R.; Koudijs, A.; Giesbers, M.; Marcelis, A. T. M.; Sudholter, E. J. R. *Liq. Cryst.* **2005**, *32*, 277.
(31) Kozmik, V.; Kovarova, A.; Kuchar, M.; Svoboda, J.; Novotna, V.; Glogarova, M.; Kroupa, J. *Liq. Cryst.* **2006**, *33*, 41.
(32) Galli, G.; Demel, S.; Slugovc, C.; Stelzer, F.; Weissflog, W.; Diele, S.; Fodor-Csorba, K. *Mol. Cryst. Liq. Cryst.* **2005**, *439*, 1909.
(33) Gallastegui, J. A.; Folcia, C. L.; Etxebarria, J.; Ortega, J.; Gimeno, N.; Ros, M. B. *J. Appl. Phys.* **2005**, *98*, 083501.
(34) Keith, C.; Reddy, R. A.; Tschierske, C. *Chem. Commun.* **2005**, 871.
(35) Chen, X.; Tenneti, K. K.; Li, C. Y.; Bai, Y.; Wan, X.; Fan, X.; Zhou, Q.-F.; Rong, L.; Hsiao, B. S. *Macromolecules* **2007**, *40*, 840.
(36) Demel, S.; Slugovc, C. F. S.; Fodor-Csorba, K.; Galli, G. *Macromol. Rapid Commun.* **2003**, *24*, 636.
(37) Choi, E-J.; Ahn, J. C.; Chien, L. C.; Lee, C. K.; Zin, W. C.; Kim, D. C.; Shin, S. T. *Macromolecules* **2004**, *37*, 71.
(38) Yariv, A. In *Optical Electronics in Modern Communications*; Oxford University Press: New York, 1997.
(39) Lee, C. K.; Kwon, S. S.; Zin, W. C.; Kim, D. C.; Shin, S. T.; Song, S.-T.; Choi, E-J.; Chien, L. C. *Liq. Cryst.* **2003**, *30*, 415.